ROBUST SLIDING MODE CONTROL BASED ON IFOC INDUCTION MACHINE WITH SPEED ESTIMATOR

Dr. Noaman M. Noaman *
Received on: 16 / 2 /2006
Accepted on: 16 / 1/2007

Abstract

In this paper, an indirect field-oriented control (IFOC) induction machine drive with a conventional PI and sliding mode controllers is presented. The robustness of ac machine drive speed performance with these controllers is checked in terms of variation of machine parameters.

The design includes rotor speed estimation from measured stator terminal voltages and currents. The estimated speed is used as feedback in an indirect vector control system, such that the speed control is performed without the use of shaft mounted transducers.

The high performance of the proposed control schemes under load disturbances is studied via simulation cases. The components of the speed controlled indirect field-oriented induction machine with the both controllers are simulated using SIMULINK, while the dynamic of induction machine is simulated using the potential of S-function block and its attached script file.

الخلاصة

في هذا البحث، تم عرض طريقتي سيطرة على سرعة مسوق القدرة، ذو سيطرة توجيه المجال الغير مباشر (IFOC Drive)، وهما استخدام مسيطر تناسبي تكاملي (PI Controller) ومسيطر النمط المنزلق (Sliding Mode Controller). تم اختبار قابلية مسوق القدرة ذو التيار المتناوب للمحافظة على قيمة السرعة، بوجود تلك المسيطرات المقترحة، وذلك من خلال إحداث تغير في معلمات الماكنة.

كذلك تضمن البحث تخمين قيمة السرعة بدون الحاجة إلى استخدام أجهزة مادية تربط مع المحرك، وتم استبدالها ببرنامج يعمل على مراقبة السرعة وتخمينها (Speed Estimator) ، وذلك من خلال قياس قيم التيارات والفولتيات الطرفية للماكنة.

تم تمثيل مكونات المنظومة المغلقة لمسوق القدرة بوجود المسيطرات المقترحة ومخمن السرعة باستخدام برنامج (Simulink) ، بينما تم الاستفادة من قابلية كتلة (S-Function Block) لغرض تمثيل انموذج الماكنة في المحاور المتعامدة (qd-Frame).

*AL-Nahrain University / College of Engineering Department of Computer Engineering

1. Introduction

Field orientation control (FOC) or vector control of induction machine achieves decoupled torque and flux dynamics leading to independent control of the torque and flux as for a separately excited DC motor [1]. This is achieved by orthogonal projection of the stator current into a torque-producing component and flux-producing component. This technique is performed by two basic methods: direct and indirect vector control. With direct field orientation, the instantaneous value of the flux is required and obtained by direct measurement using flux sensors or flux estimators, whereas indirect field orientation is based on the inverse flux model dynamics, and there are three possible implementation based on the stator, rotor, or air gap flux orientation. The rotor flux indirect vector control technique is the most widely used due to its simplicity [2]. FOC methods are attractive but suffer from one major disadvantage. They are sensitive to parameter variations such as rotor time constant and incorrect flux measurement or estimation at low speeds. Consequently, performance deteriorates and a conventional controller such as a PI is unable to maintain satisfactory performance under these conditions [1].

A sliding mode control (SMC) is basically an adaptive control scheme that gives robust performance of a drive with parameter variations. The control is nonlinear and applied to linear and nonlinear plant. In SMC, the drive response is forced to slide along a predefined trajectory in a phase plane by a switching control algorithm, irrespective drive's parameter variation and load disturbance [3, 4].

Controlled induction motor drives without mechanical speed sensors at the motor shaft have the attractions of low cost and high reliability. To replace the sensor, the information on the rotor speed is extracted from measured stator voltages and currents at the motor terminals. Vector-controlled drives require estimating the magnitude and spatial orientation of the fundamental magnetic flux waves in the stator or in the rotor [4, 5].

In this paper, two control strategies are considered to adjust the speed of the drive system: PI and sliding mode controller. The robustness of these suggested controllers are checked in terms of motor parameter variations. The speed controller is performed under no mechanical speed sensors and speed observer, based on the software program, is adopted for this purpose.

2. Dynamic Model of Induction Machine

Induction machine (IM) equations in arbitrary rotating reference frame can be represented in stator and rotor dq voltage equations [5-8]:

$$v_{qs} = p\lambda_{qs} + \omega\lambda_{ds} + r_s i_{qs}$$

$$v_{ds} = p\lambda_{ds} - \omega\lambda_{qs} + r_s i_{qs}$$

$$v'_{qr} = p\lambda'_{qr} + (\omega - \omega_r)\lambda'_{dr} + r'_r i'_{qr}$$

$$v'_{dr} = p\lambda'_{dr} - (\omega - \omega_r)\lambda'_{qr} + r'_r i'_{qr}$$

(1)

Where v is voltage; λ is the flux linkage; i is the current; ω is the arbitrary speed of the reference frame; r is the resistance and p is the time derivative. The subscript r and s denotes the rotor and stator values respectively referred to the stator, and the subscripts

d and *q* denote the dq-axis components in the arbitrary reference frame.

The equations of the machine in the stationary and synchronously rotating reference frame can be obtained from (1) by setting ω to zero and $\omega = \omega_e$, respectively. To distinguish these two frames from each other, an additional superscript will be used; *s* for stationary frame variables and *e* for synchronously rotating frame variables.

The electromagnetic torque equation can be given by [5, 6]

$$T_{em} = \frac{3}{2}\frac{P}{2}(\lambda'_{qr}i'_{dr} - \lambda'_{dr}i'_{qr})$$

(2)

where P denotes the number of machine pole pairs. Using Eq.(1) and (2), one can obtain the state-space model for induction motor developed in stationary reference frame as given below

$$[5,9,10]: \frac{d}{dt}\begin{bmatrix} i^s_{ds} \\ i^s_{qs} \\ \lambda'^s_{dr} \\ \lambda'^s_{qr} \\ \omega_r \end{bmatrix} =$$

$$\begin{bmatrix} -\dfrac{K_R}{K_L} & 0 & \dfrac{L_m r'_r}{L_r^2 K_L} & \dfrac{L_m \omega_r}{L_r K_L} & 0 \\ 0 & -\dfrac{K_R}{K_L} & -\dfrac{L_m \omega_r}{L'_r K_L} & \dfrac{L_m r'_r}{L_r'^2 K_L} & 0 \\ \dfrac{L_m}{T_r} & 0 & -\dfrac{1}{T_r} & -\omega_r & 0 \\ 0 & \dfrac{L_m}{T_r} & \omega_r & -\dfrac{1}{T_r} & 0 \\ -K_M \lambda'^s_{qr} & K_M \lambda'^s_{dr} & 0 & 0 & B \end{bmatrix}$$

$$\begin{bmatrix} i^s_{ds} \\ i^s_{qs} \\ \lambda^s_{dr} \\ \lambda^s_{qr} \\ \omega_r \end{bmatrix} + \frac{1}{K_L}\begin{bmatrix} 1 & 0 & 0 \\ 0 & 1 & 0 \\ 0 & 0 & 0 \\ 0 & 0 & 0 \\ 0 & 0 & -K_L \end{bmatrix}\begin{bmatrix} V^s_{ds} \\ V^s_{qs} \\ T_L \end{bmatrix} \quad (3)$$

$$\begin{bmatrix} i^s_{ds} \\ i^s_{qs} \end{bmatrix} = \begin{bmatrix} 1 & 0 & 0 & 0 & 0 \\ 0 & 1 & 0 & 0 & 0 \end{bmatrix}\begin{bmatrix} i^s_{ds} \\ i^s_{qs} \\ \lambda'^s_{dr} \\ \lambda'^s_{qr} \\ \omega_r \end{bmatrix} +$$

$$\begin{bmatrix} 0 & 0 \\ 0 & 0 \end{bmatrix}\begin{bmatrix} V^s_{ds} \\ V^s_{qs} \end{bmatrix}$$

(4)   where $K_L = (L_r L_s - L_m^2)/L'_r$,

$K_R = r_s + r'_r(L_m/L'_r)^2$ and

$K_M = (3P^2 L_m)/(8JL'_r)$ .The

parameters L'_r, L_s, L_m are rotor, stator and main inductances, respectively. $T_r = L_r/r'_r$ is the rotor time constant; B is the viscous friction coefficient; J is the inertia constant of the motor; T_L is the external load; ω_r is the rotor electrical speed in angular frequency.

3. Indirect Field Orientation Control (IFOC)

Indirect vector control is very popular in industrial applications. Figure (1) explains the fundamental principle of indirect vector control with the help of a phasor diagram. The $d^s - q^s$ axes are fixed on the stator, but the $d^r - q^r$ axes, which are fixed on the rotor, are moving at speed ω_r. Synchronously rotating axes $d^e - q^e$ are rotating ahead of the $d^r - q^r$ axes by the positive slip angle θ_{sl} corresponding to slip frequency ω_{sl}.

Since the rotor pole is directed on the d^e axis and $\omega_e = \omega_r + \omega_{sl}$, one can write

$$\theta_e = \int \omega_e dt = \int (\omega_r + \omega_{sl}) dt = \theta_r + \theta_{sl}$$

(5)

of control equations of indirect vector control with the help of $d^e - q^e$ dynamic model of IM ,i.e., using Eq.(1) with the addition of superscript e to the variables and setting $\omega = \omega_e$ .If $d^e - axis$ is aligned with the rotor field, the q-component of the rotor field, $\lambda_{qr}^{\prime e}$, in the chosen reference frame would be zero. One can easily show the following important equations;

$$T_{em} = \frac{3}{2} \frac{P}{2} \frac{L_m}{L_r} \lambda_{dr}^{\prime e} i_{qs}^e$$

(6)

$$\lambda_{dr}^{\prime e} = \frac{r_r' L_m}{r_r' + L_r' p} i_{ds}^e$$

(7)

$$\omega_{sl}^e = \omega_e - \omega_r = \frac{r_r'}{L_r'} \frac{i_{qs}^e}{i_{ds}^e}$$

(8)

To implement the indirect vector control strategy, it is necessary to use the condition in Eq.s (6), (7), and (8) in order to satisfy the condition for proper orientation. Figure (2) shows an indirect field-oriented control scheme for a current controlled PWM induction machine motor drive.

The command values for the *abc* stator currents can then be computed as follows

$$i_{qs}^{s*} = i_{qs}^e \cos\theta_e + i_{ds}^e \sin\theta_e$$

$$i_{ds}^{s*} = -i_{qs}^e \sin\theta_e + i_{ds}^e \cos\theta_e$$

(9)

The phasor diagram suggests that for decoupling control, the stator flux component of current i_{ds}^e should be aligned on the d^e axis, and the torque component of current i_{qs}^e should be on the q^e axis, as shown. For decoupling control, one can make a derivation

$$i_{as}^* = i_{qs}^{s*}$$

$$i_{bs}^* = -(1/2)i_{qs}^{s*} - (\sqrt{3}/2)i_{ds}^{s*}$$

$$i_{cs}^* = -(1/2)i_{qs}^{s*} + (\sqrt{3}/2)i_{ds}^{s*}$$

(10)

4. Motor Speed Calculation

Figure (2) shows the connection of the speed estimator with IFOC IM. The block calculates the synchronous and rotor speed based on the measurements of line voltages and currents. Starting from the flux equations [1, 4]

$$\lambda_s^s = L_s i_s^s + L_m i_r^{\prime s} ,$$

$$\lambda_r^s = L_m i_s^s + L_r' i_r^{\prime s}$$

(11)

the expressions for λ_s^s and i_r^s can be obtained as

$$\lambda_s^s = \frac{L_m}{L_r'} \lambda_r^{\prime s} + \sigma L_s i_s^s ,$$

$$i_r^{\prime s} = \frac{1}{L_r'}(\lambda_r^{\prime s} - L_m i_s^s)$$

(12)

Substituting of (12) in the drive voltage equations, Eq.(1), gives

$$V_s^s = r_s i_s^s + s\lambda_s^s ,$$

$$V_r^s = r_s i_r^{\prime s} + (s - j\omega)\lambda_r^{\prime s}$$

(13)

Hence

$$s \begin{bmatrix} \lambda_{dr}^{\prime s} \\ \lambda_{qr}^{\prime s} \end{bmatrix} =$$

$$\frac{L'_r}{L_m}\left(\begin{bmatrix} V^s_{ds} \\ V^s_{qs} \end{bmatrix} - \begin{bmatrix} r_s + s\sigma L_s & 0 \\ 0 & r_s + s\sigma L_s \end{bmatrix}\begin{bmatrix} i^s_{ds} \\ i^s_{qs} \end{bmatrix}\right)$$

(14)

$$s\begin{bmatrix} \lambda'^s_{dr} \\ \lambda'^s_{qr} \end{bmatrix} =$$

$$\frac{1}{T_r}\left(L_m\begin{bmatrix} i^s_{ds} \\ i^s_{qs} \end{bmatrix} - \begin{bmatrix} 1 & \omega T_r \\ -\omega T_r & r_s + s\sigma L_s \end{bmatrix}\begin{bmatrix} \lambda^s_{ds} \\ \lambda^s_{qs} \end{bmatrix}\right)$$

(15)

where $\sigma = 1 - (L^2_m/L'_r L_s)$ and s is the Laplace operator. Equations (14) and (15) represent the rotor flux observers and are termed the voltage model and the current model, respectively. The rotor flux amplitude and phase are

$$\lambda_r = \sqrt{(\lambda^s_{dr})^2 + (\lambda^s_{qr})^2} \text{ , and}$$

$$\theta_r = \tan^{-1}\left(\frac{\lambda'^s_{qr}}{\lambda'^s_{dr}}\right)$$

(16)

Differentiating (16) and substituting (15) leads to the drive speed

$$\omega_r = \omega_e - \frac{L_m}{T_r \lambda'^2_r}(i^s_{qs}\lambda'^s_{dr} - i^s_{ds}\lambda'^s_{qr})$$

$$=$$

$$\frac{1}{\lambda'^2_r}\left[(\lambda'^s_{dr}\dot{\lambda}'^s_{qr} - \lambda'^s_{qr}\dot{\lambda}'^s_{dr} - \frac{L_m}{T_r}(\lambda'^s_{dr}i^s_{qs} - \lambda'^s_{qr}i^s_{ds})\right]$$

(17)

Therefore, given a complete knowledge of the motor parameters, the instantaneous speed ω_r can be calculated from Eq.(17), where the voltage model of Eq.(14) is used to estimate the rotor flux amplitude.

5. Sliding Mode Control

With the proper field orientation and with rated rotor flux, the torque equation, Eq.(6), can be rewritten as [1]

$$T_{em} = K_T i^e_{qs}$$

(18)

where K_T is the torque constant, and is defined as follows

$$K_T = \frac{3}{2}\frac{P}{2}\frac{L_m}{L'_r}\lambda'^{*e}_{dr}$$

(19)

where λ'^*_{dr} denotes the command rotor flux. The mechanical equation of an induction motor can be written as [5,6]:

$$J\dot{\omega}_m + B\omega_m + T_L = T_{em}$$

(20)

where $\omega_m = (2/P)\omega_r$ is the rotor mechanical speed. Using Eq.(18), one can obtain

$$\dot{\omega}_m + a\omega_m + f = bi^e_{qs}$$

(21)

where,

$$a = B/J , b = K_T/J ,$$

$$f = T_L/J$$

(22)

Eq.(21) can be written with uncertainties $\Delta a, \Delta b$ and Δf in the terms a, b, and f respectively, as follows:

$$\dot{\omega}_m = (a + \Delta a)\omega - (f + \Delta f) + (b + \Delta b)i^e_{qs}$$

(23)

The tracking speed error can be defined as,

$$e(t) = \omega_m(t) - \omega^*_m(t)$$

(24)

where, ω^*_m is the rotor speed command. Taking the derivative of Eq.(24) with respect to time yields:

$$\dot{e}(t) = \dot{\omega}_m - \dot{\omega}^*_m = -ae(t) + u(t) + d(t)$$

(25)

where the following terms have been collected in the signal $u(t)$,

$$u(t) = bi_{qs}^e - a\omega_m^*(t) - f(t) - \dot{\omega}_m^*(t)$$
(26)

and the uncertainty terms have been collected in the signal $d(t)$,

$$d(t) = -\Delta a\omega_m(t) - \Delta f(t) + \Delta bi_{qs}^e(t)$$
(27)

The sliding variable S(t) can be defined with an integral component as:

$$S(t) = e(t) - \int_0^t (k-a)e(\tau)d\tau$$
(28)

where k is a constant gain.

When the sliding mode occurs on the sliding surface of Eq.(28), then $S(t) = \dot{S}(t) = 0$, and therefore dynamic behavior of the tracking problem (Eq.(25)) is equivalently governed by the following equation:

$$\dot{S}(t) = 0 \quad \Rightarrow \quad \dot{e}(t) = (k-a)e(t)$$
(29)

In order to obtain the speed trajectory tracking the following assumption should be formulated [4]:

❑   The gain k must be chosen so that the term *(k-a)* is strictly negative, therefore

(k<0).Then the sliding surface is defined as:

$$S(t) = e(t) - \int_0^t (k-a)e(\tau)d\tau = 0$$
(30)

The variable structure speed controller is designed as:

$$u(t) = ke(t) - \beta \operatorname{sgn}(S)$$
(31)

where the k is the gain defined previously, β is the switching gain, sgn(.) is

signum function.

❑   The gain β must be chosen so that $\beta \geq |d(t)|$.

The   current   command i_{qs}^* , can be obtained directly substituting Eq.(31) in Eq.(26):

$$i_{qs}^*(t) = \frac{1}{b}\left[ke - \beta \operatorname{sgn}(S) + a\omega_m^* + \dot{\omega}_m^* + f\right]$$
(32)

Therefore, the proposed variable structure speed control resolves the speed-tracking   problem   for   the induction   motor,   with   some uncertainties in mechanical parameters and load torque.

6. Modeling of PI and Sliding Mode Control-Based IFOC IM

Referring to Eq.(6), the stator quadrature-axis current reference i_{qs}^* is calculated from torque reference T_{em}^* as:

$$i_{qs}^* = \frac{2}{3}\frac{2}{P}\frac{L_r'}{L_m}\frac{T_{em}^*}{\lambda'^*_r}$$
(33)

The stator direct-axis current reference i_{qs}^* is calculated from rotor flux linkage reference λ_r^* using,

$$i_{ds}^* = \frac{(L_r'p\lambda_r^* + r_r'\lambda_r^*)}{r_r'L_m}$$
(34)

The rotor flux position θ_e is generated from synchronous speed ω_e integration, which   estimated   from   the   estimator block.

Equations   (33)   and   (34) represent   the   main   equations responsible for field oriented-control, which   is   represented   by   the   Field Oriented   block   diagram   shown   in Fig.(3)

The conversion of quantities from dqe to abc reference frames are executed by dq_abc block,
The quantities in abc reference frame are converted to dqs frame using Fig.(5),
The speed controller with the proportional-integral type can be implemented using Simulinks blocks

The modeling of the elements of the sliding mode controller is shown if Fig.(7)
The current regulator, which consists of three hysteresis controllers, is built with Simulink blocks. The motor currents are provided by the multiplexer output of the induction machine block,
The simulation block diagram for a three-phase, two-level PWM inverter is shown below.

Each leg of the inverter is represented by a "switch" which has three input terminals and one output terminal. The output of the switch oscillates between $(+0.5 V_{dc})$ and $(-0.5\ V_{dc})$, which is characteristic of a pole of an inverter.

$$v_{an} = (2/3)v_{ao} - (1/3)v_{bo} - (1/3)v_{co}$$

$$v_{bn} = (2/3)v_{bo} - (1/3)v_{ao} - (1/3)v_{co}$$
(35)

$$v_{cn} = (2/)v_{co} - (1/3)v_{ao} - (1/3)v_{bo}$$

The SIMULINK modeling of speed observer based on Eq.(17) is illustrated in Fig.(10)

Block diagrams of Figs.(3)-(10) can be assembled to yield the block diagram of PI or sliding mode controller-based IFOC I.M. , which is given in Fig.(11)

7. Simulated Results

In this section the speed regulation performance of the proposed sliding mode is compared to that of the PI controller of the field oriented control IM. The performance is checked in terms of load torque variations. The simulation is performed in SIMULINK, while the IM model is simulated using s-function block after dicretizing the IM model defined in Eq.s(3) and (4). The IFOC IM of Fig.(11) is run at sampling period $T_s = 2e - 6$. The IM used in this case study has the parameters listed in table (1)

In the following study, the variation of the motor parameters is confined to load change only, while the other parameters, e.g. viscous friction B, are held constant.

In the first test, the PI controller is used as a speed controller and a cyclic change of different load torque levels are subjected to the machine at certain times and as follows:
Time = [0 0.75 0.75
1.0 1.0 1.25 1.25 1.5 1.5 2];
Torque = [0   0   -10
-10 –5   –5   5   5   0   0];
The responses of speed, developed torque, and stator current are shown in Fig.(12). It is evident from the figure that the PI controller shows bad speed response at these applied changes of loads and lacks the ability to hold the speed at the required value. Therefore, it is true to say that the PI controller is not robust against the changes of IM parameters. Retuning of the PI parameters may slightly reduce the change of speed due to its corresponding change of load.

In the second test, the sliding mode controller is proposed and a change of ± 20 N.m of load applied for a period of time. For this value of load level change β is found to be 8, and the value of k is set to be 100. The value

of β limits the value of exerted load, while the value of k determines the speed of tracking according to Eq.(34). The form of this repeated load change can be clarified as follows:

$$\text{Time} = [0 \quad 0.75 \quad 0.75 \quad 1.0 \quad 1.0 \quad 1.25 \quad 1.25 \quad 1.5 \quad 1.5 \quad 2];$$
$$\text{Torque} = [0 \quad 0 \quad -20 \quad -20 \quad 0 \quad 0 \quad 20 \quad 20 \quad 0 \quad 0];$$

where the load is exerted in time ranges [0.75 - 1.0] and [1.25 - 1.5]. The speed response of Fig.(13) shows no detected change in the rotor speed at these ranges, meaning that the sliding mode controller does well in rejecting the applied torque; therefore the rotor speed is by now riding over the sliding trajectory and the controller is robust against IM parameter variations.

To which extent the controller can reject the applied load depends on the value β, which has been determined based on the load level. In the above case, the value of β has been calculated to be greater than 8 for the sliding mode controller to reject the load levels less (greater) than 20 (-20). Otherwise the controller begins to lack the ability to reject the values of load level greater than 20 (or less than –20) unless the boundary of β is increased over the previous one (8). The strong evident of this argument is clearly shown in Fig.(14), where the exerted load level exceeded 20 N.m while the value of β is held constant at the value 8. The speed response deteriorates and a change in the rotor speed will appear at time of exerting ± 25 N.m. Therefore the boundary of β should be released and should have a new value other than 8 for the controller to manage the new level of load change.

8. Conclusion

From the simulated results the following points can be concluded:

❑ The PI controller is not robust against IM parameter variations, and as has been shown the speed response degrades to different level of load changes.

❑ The sliding mode controller can overcome the problem of system degradation, encountered in PI controller, on the condition that the sliding mode controller is well designed for the specified level of load changes.

❑ If the load level exceeds the design specification, degradation in the speed response is observed unless another design procedure is adopted.

References

[1] M. A. Denai and S. A. Attia,"**Fuzzy and Neural Control of an Induction Motor,**" Int. J. Appl. Math. Comput. Sci, Vol.12, No. 2, p 221-233, 2002.

[2] M. A. Denai and S. A. Attia, "**Intelligent Control of an Induction Motor,**" Int. J. Electric Power Components and System, 30:409-427, Taylor and Francis Ltd, 2002.

[3] Christopher Edwards and Sarah K. Spurgeon, "**Sliding Mode Control: Theory and Application,**" Taylor and Francis Ltd, 2002.

[4] O. Barambones, A. J. Garrido and F. J. Maseda,"**A Sensorless Robust Vector Control of Induction Motor Drives,**" University of Pais Vasco, 2002.

[5] Bimal K. Bose, "**Modern Power Electronics and AC Drive,**" University of Tennessee, Knoxville, Prentice Hall, 2001.

[6] Chee-Mun Ong, "**Dynamic Simulation of Electric Machinery Using Matlab/Simulink**", Purdue University, Prentice Hall PTR, 1998.

[7] Dal Y. Ohm, "**Dynamic Model of Induction Motors for Vector Control**", Drivetech, Inc., Blacksburg, Virginia, 2001.

[8] W. Leonhard ," **Control of Electrical Drives,**" Springer Press, Berlin, 1996.

[9] A. Ouhrouche and C. Volat, "**Simulation of a Direct Field-Oriented Controller for an Induction Motor Using MATLAB/SIMULINK Software Package**", Proceeding of the IASTED International Conference Modeling and Simulation, Pennsylvania, USA, May 15-17, 2000.

[10] Bilal Akin, "**State Estimation Techniques for Speed Sensorless Field Oriented Control of Induction Machine**", Master's thesis, The Middle East technical university, 2003.

[11] *Math Works, Inc., "SIMULINK user's Guide," Version 2, Jan 1997.*
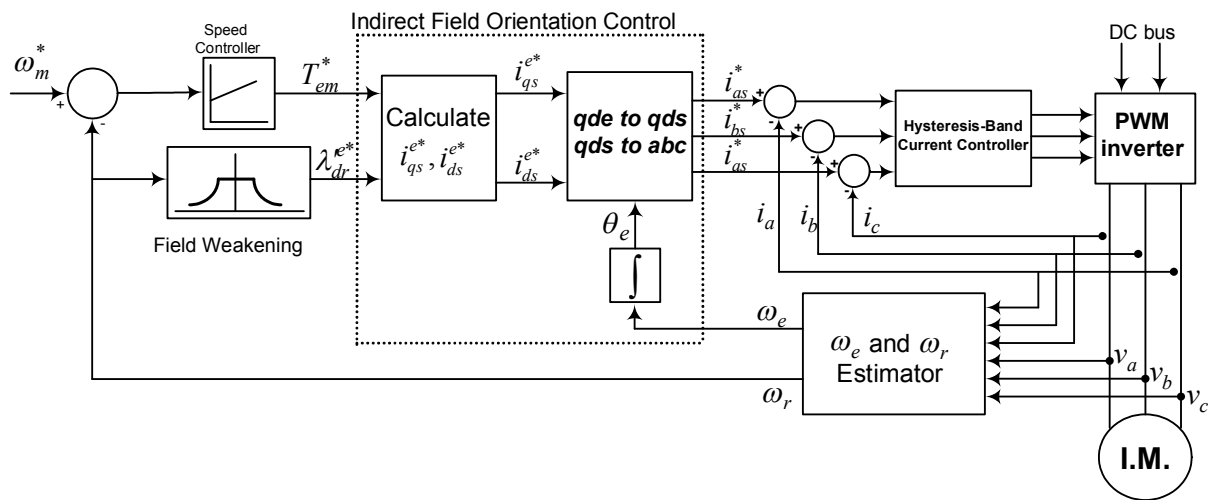
Figure (1) indirect field-Oriented control of a current regulated **PWM** inverter induction motor drive
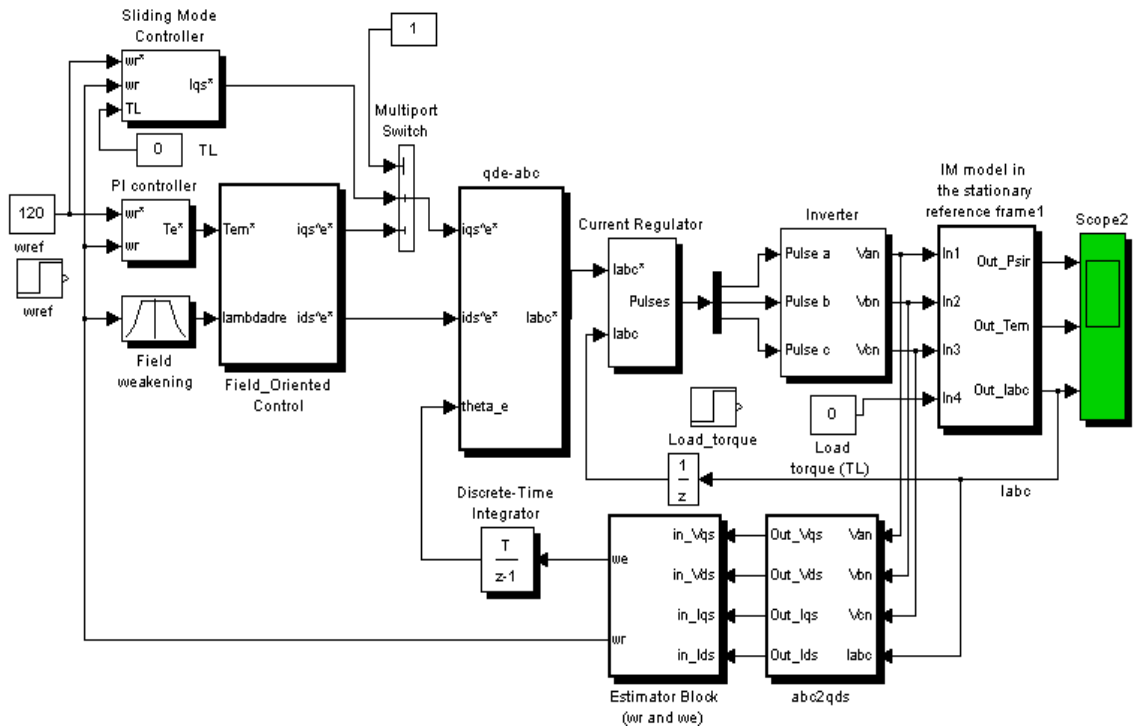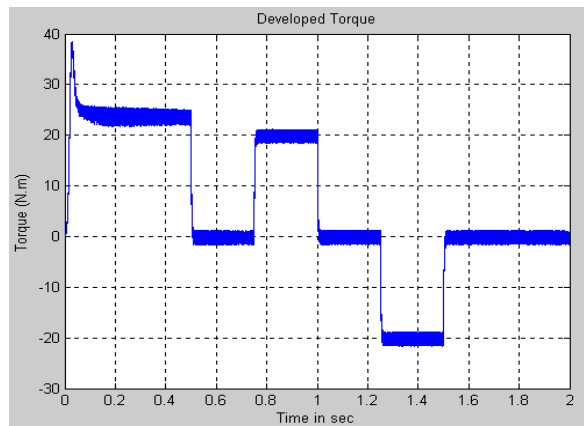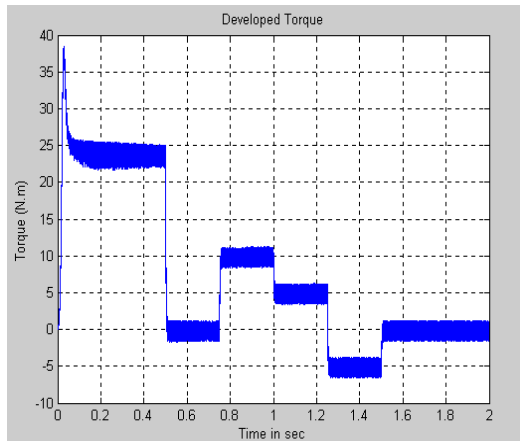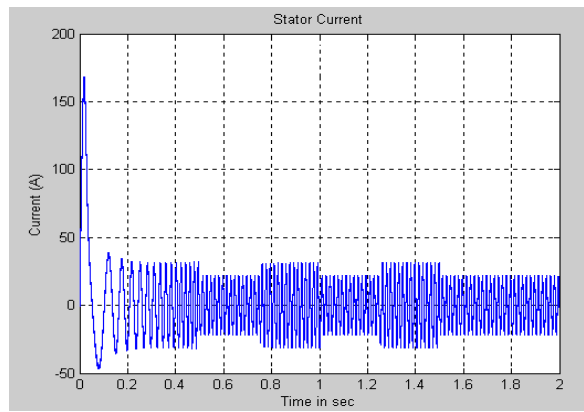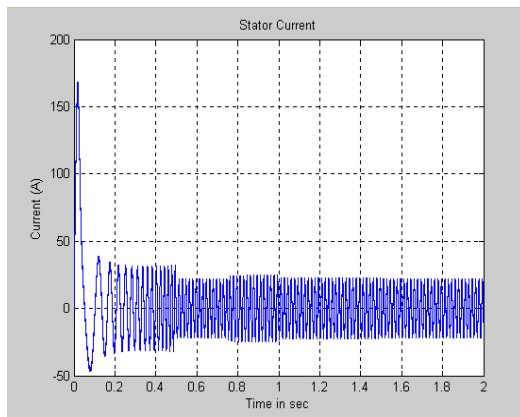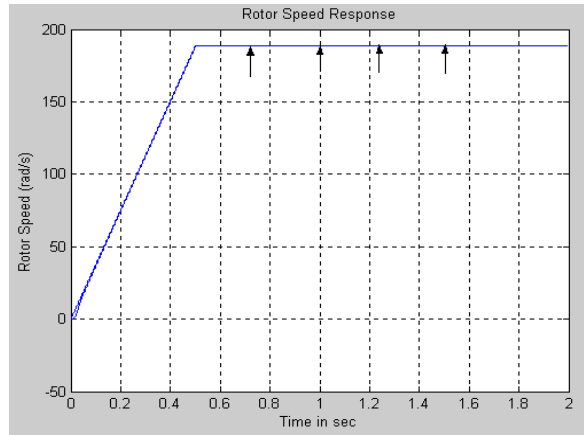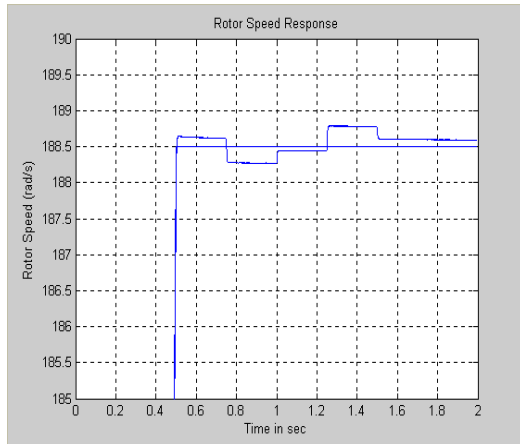
Figure (2) SIMULINK modeling of PI and sliding Mode Control-Based IFOC IM

Table 1: Induction Motor Parameter

Rated Power	20 hp
Rated Line-Line Voltage	200 V
Rate Torque	81.5 Nm
Number of Pole pairs (P)	2
Stator Resistans (rs)	0.106 Ω
Stator Inductance (L_s)	9.15 mH
Magnetizing Inductance(L_m)	8.67 mH
Rotor Resistance (r_r)	0.076 Ω
Rotor Inductance (L_r)	9.15 mH

Figure (3) PI control-Based IFOC
 Induction Machine

Figure (4) Sliding mode control-Based
   IFOC Induction Machine

Figure (5) Sliding mode control-Based **IFOC** Induction Machine When higher levels of torque load are exerted